

MEASUREMENT OF A SIDE-WALL BOUNDARY EFFECT IN SOIL COLUMNS USING FIBRE-OPTICS SENSING

P. SENTENACⁱ⁾, R.J. LYNCHⁱⁱ⁾ AND M.D. BOLTONⁱⁱⁱ⁾

ABSTRACT

Side-wall leakage - the preferential flow of water or pollutants near the wall of a soil column - has been studied using in-situ fibre-optical detection of a dye solution at the boundary and in the centre of a soil column. A difference in flow velocity was clearly observed between centre and column wall boundary for different surfaces. The velocity difference is modified by sand-coating of the wall surface.

Key words: flow, sand, tracer, hydraulic gradient

INTRODUCTION

Laboratory experiments for investigating the permeability of soils or contaminant transport often involve the study of a flow of water through soil columns held in tubes of steel, glass or other rigid material. There is often thought to be a boundary effect or side-wall leakage associated with such columns, i.e. the local permeability of the soil at the interface with the tube is greater than the permeability at the centre of the column. Flexible walled permeameters have been used to overcome such effects (e.g. Daniel et al., 1985).

Nevertheless because of their simplicity, many experiments on permeability or contaminant transport are carried out in rigid tubes. Poorooshasb and Schofield (1988) studied the density driven flow of salt contaminant in a rigid walled column of silt at increased gravity in a centrifuge. They found evidence of fingering (increased flow) near the wall when the contaminant was moving down through unsaturated soil. In studies of contaminant transport of NAPLs (non-aqueous pollutant liquids), fingering has been reduced near the window of a centrifuge soil sample by sand blasting of the glass (Spiessl and Taylor, 2000). Budhu (1991) has compared results of organic permeation in rigid walled and flexible walled permeameters. In most cases, soil permeability ratios of organic/water were greater for the rigid wall permeameter, suggesting side-wall leakage effects.

In a study of the flow of water through plate-like wood chips, as used in paper pulp making, evidence of a wall effect was found (Comiti and Renaud, 1989). They proposed two reasons: a change in the viscous resistance, due to a difference in the surface roughness between the wall and a particle, and also a reduction in tortuosity near the wall.

In this laboratory we are currently studying the transport of water-soluble contaminants through soils and simulated landfill liners using fibre-optic sensors. We have used these sensors to track the movement both of a dye tracer and of copper salt in 1-dimensional experiments (Treadaway et al., 1997). We also have applied this technology to contaminant transport studies in geotechnical centrifuge experiments (Treadaway et al., 1998, Lynch et al., 2000). Using similar technology it was decided to measure the boundary effect by measuring the time differences at which a plume of water-soluble dye passes sensors at the wall and at the centre of a column of soil.

EXPERIMENTAL PROCEDURE

The experimental apparatus is shown in Fig. 1. The soil sample is contained in a rigid plastic Perspex tube, 120 mm outer diameter and 200 mm deep. Below the soil is a 20 mm layer of gravel retained by porous plastic sheet. The surface of the soil is covered by another sheet of porous plastic. This avoids disturbance of the surface by the incoming stream of water. Apart from the time of the plume injection, the water level is maintained constant 10 mm above the soil by means of an electronically operated solenoid valve, controlled by the dry/wet resistance of two stainless steel pins. The outlet of the soil container is to a tap of adjustable height, to provide a range of hydraulic gradients.

Preparation of the fully saturated soil sample

The tube is filled with de-aired water and sand of particle size 300-600 μ m (fraction C) or 600-1200 μ m (fraction B), (David Ball & Co., Lolworth, Cambs). Sand is introduced into the water by keeping it fully saturated

i) Department of Chemical Engineering, The University of Bath, Bath BA27 AY, UK.

ii) Senior Technical Officer, Geotechnical group, Cambridge University Engineering Department, Cambridge CB 2 1PZ, UK.

iii) Professor, ditto.

Manuscript was received for review on November 22, 2001.

from a bucket containing soil and de-aired water. A 3 mm thickness piece of porous plastic is de-aired in water and then covers the sand. This procedure is more accurate than using filter paper, which does not prevent water flow soil disturbance. After the sample is loaded, the model is consolidated using a shaking table.

Release of the dye plume

The dye is prepared by diluting the concentrate, (Raynor's green food colouring, Middlesex), to 1% by volume. At first, steady state conditions are established in the column, with a constant head of water. When flat baseline conditions are observed from the sensors, the plume injection is carried out in the following manner: The water level is allowed to fall until the soil surface is almost exposed. 60 ml of green dye solution is poured evenly into the water above the porous plastic, and allowed to pass into the soil. When the dye has almost completely entered the soil, water flow is resumed and controlled at a constant head by means of the water level controller which operates the water tank solenoid valve, and keeps the hydraulic gradient constant.

Sensors

Three photometric optical fibre sensors have been used in this work (Lynch et al., 2001):

1. A light-transmission type described previously, (Treadaway, et al., 1997), shown in Fig. 2 (a), in which light from a light emitting diode passes through the pore fluid; the transmitted light is measured by a photodiode circuit.

2. Two light-reflection types are also shown in Fig. 2(b, c). In these sensors the light from a light-emitting diode

is transmitted by a fibre to the soil sample. It passes through the voids, is reflected from the soil surfaces, and collected by another fibre. Optionally a layer of geotextile mesh can be used to increase the void space. This has the effect of increasing substantially the sensitivity but at the penalty of increasing the response time, since there will be a time associated with this mesh chamber filling and emptying of dye. In these experiments no mesh chamber was used. The fibres used in the transmission type are standard step-index fibre of 1 mm core diameter and 2.2 mm outer diameter. In the "bi-fibre" type, the plastic cladding was stripped from two 1 mm fibres and the two cores glued together so that the fibres were parallel and the ends level. A thin shrink-wrap sleeving was applied to the fibres. This small, un-intrusive sensor can be applied with minimal disturbance to the soil. In this experiment they were located 90 mm below the soil surface.

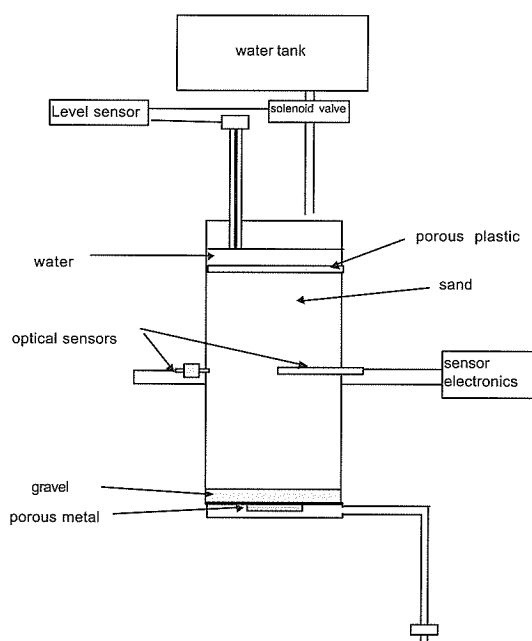
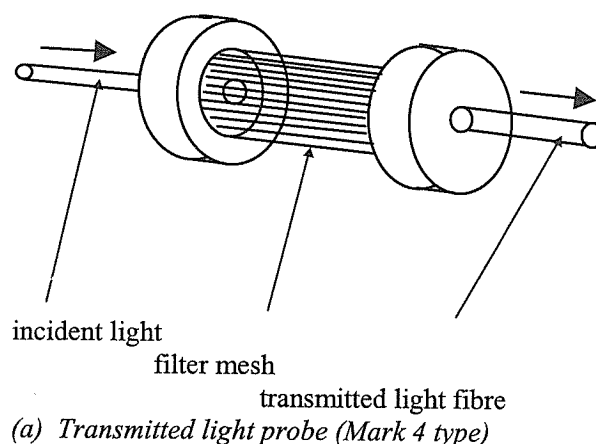


Fig. 1. Experimental arrangement

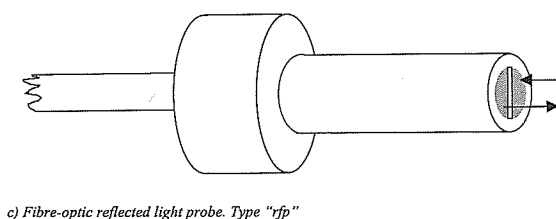
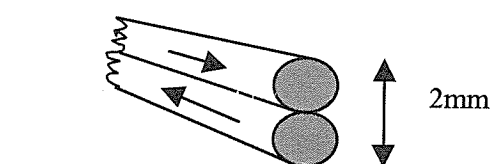


Fig. 2. Fibre-optic photometric sensors

Electronics

The two sensors are connected to an electronic circuit which provides the following functions:

1. Light emitting diodes and associated power supplies;
2. Photodiodes for measuring received light intensity;
3. Logarithmic amplifiers which allow the output voltage to vary linearly with dye concentration, according to Beer's Law (light absorbance equals $\log(1/\text{transmittance})$, which is proportional to dye concentration),
4. A differential amplifier which compares the light intensity changes in sample and reference sensors.

The output signals are stored in a data logger (Handy-scope) connected to a personal computer. Details of the electronics system have been described previously (Treadaway, et al., 1997, 1998).

RESULTS AND DISCUSSION:

Sensor calibration

The sensors were calibrated at increasing concentrations of dye, measured with the sensors in position in the soil. Fig. 3 shows the calibration plots for the two sensors, i.e. the output voltage at various concentrations of dye. The packing of the soil grains around these reflective probes could affect the calibration, so both soil types were used. In fact, the slopes of the linear regression fit did not vary significantly. It is recognised that a potential problem with this method of calibration is that there may be adsorption of the dye onto the soil particles surfaces,

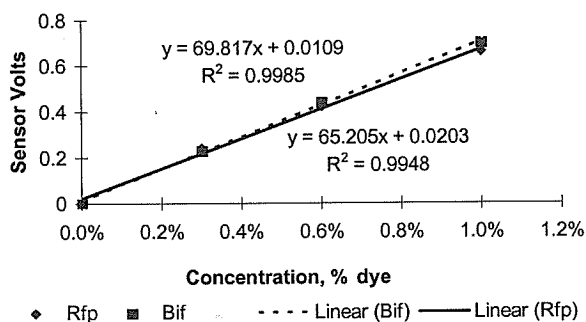


Fig. 3(a). Sensors calibration plot in Soil B

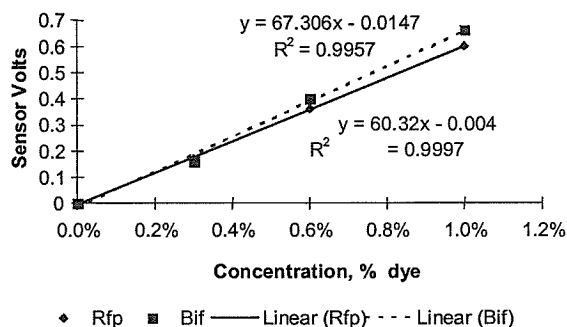


Fig. 3(b). Sensors calibration plot in Soil C

so that the concentration sensed by the fibre is reduced. However in this case there appears to be little adsorption of the dye by the sand, and the linear nature of the calibration plots agrees with Beer's Law.

Rigid, uncoated column walls

Figure 4 shows the plumes detected by two sensors of the reflective type, mounted at the edge and at the centre (on the axis) of a column of Fraction B sand (0.6-1.2 mm particle size range).

The sensor at the edge was mounted with the sensitive surface mounted level with the column wall. Fig. 5 shows similar plumes in Soil C (300-600 μm particle diameter).

It is clear that in both cases the plume at the edge leads that at the centre. In Soil B the difference is about 50% of the plume width and in soil C, 26% of the plume width. At the soil/wall interface the local voids ratio may be larger than elsewhere in the soil, and this would be consistent with the plume travelling faster near the column walls.

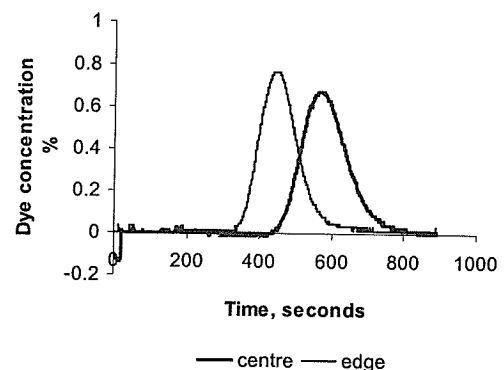


Fig. 4. Plume at centre and wall of column (sand B, uncoated wall, 0.77 hydraulic gradient)

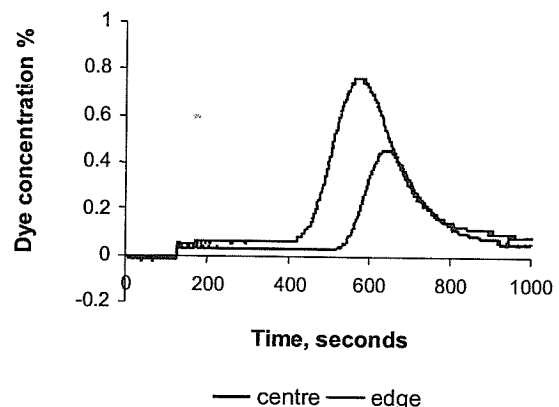


Fig. 5. Plume at centre and wall of column (sand C, uncoated wall, 0.77 hydraulic gradient)

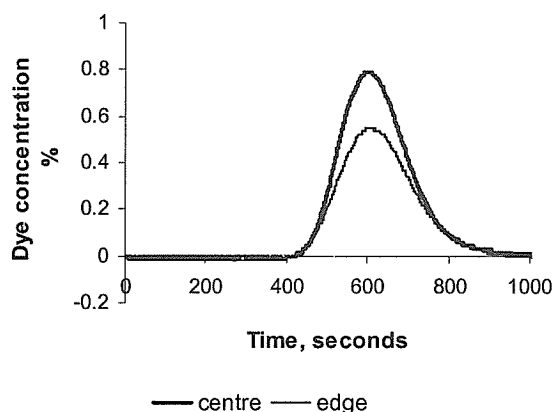


Fig. 6. Plume at centre and wall of column (sand B, 0.77 hydraulic gradient, coated wall)

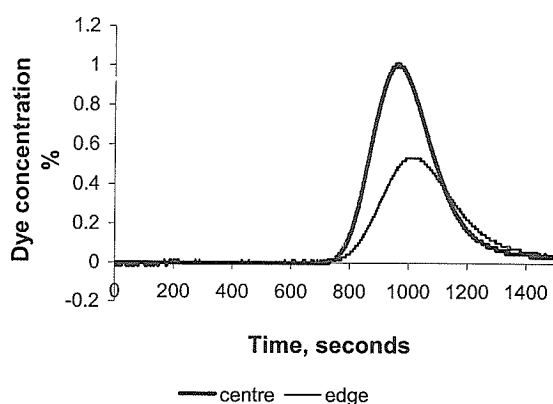


Fig. 7. Plume at centre and wall of column (sand C, 0.77 hydraulic gradient, coated wall)

Modified column walls

The column wall was then coated with double-sided adhesive tape and coated with the same sand on test. In this series the plume of dye at the edge is now retarded by the effect. Figures 6 and 7 show the results collected at the same hydraulic gradient as Figs. 4 and 5 above but with coated walls.

The plume at the edge now can be seen to coincide (Fig. 6) or even to trail behind (Fig. 7) that of the centre, in contrast to the uncoated wall results. This seems entirely reasonable since the sand-coating of the walls has reduced the relative disturbance to the packing at the edge, and reduced the local increase in voids ratio. An alternative explanation is perhaps that there is now an affinity between the dye and column surface. A reduction in flow rate also accompanied the column wall coating.

Figures 4-7 were all obtained at a constant hydraulic gradient of 0.77. These simple experiments suggest that the boundary effect is increased with larger soil particle sizes. This is difficult to explain since the suggested mechanism is dependent on packing geometry rather than grain size.

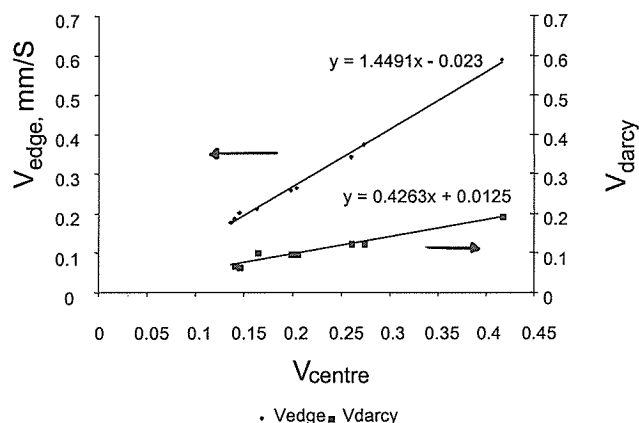


Fig. 8. Velocity at the edge and Darcy velocity vs. velocity at the centre, mm/S; Soil B

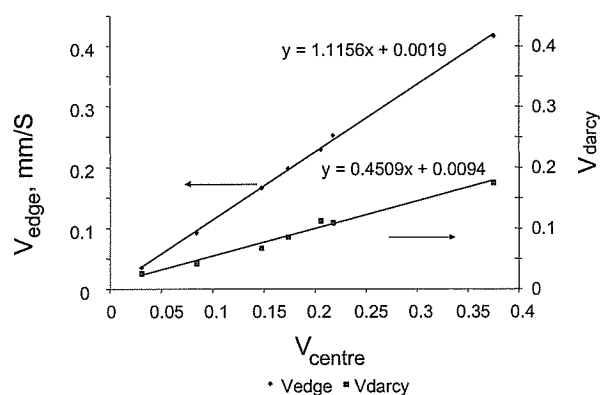


Fig. 9. Velocity at the edge and Darcy velocity vs. velocity at the centre, mm/S; Soil C

The measurements indicate that the delay is more exaggerated at small hydraulic gradients. In Fig. 8, the velocity at the edge measured by the edge-mounted sensor, v_{edge} , is plotted against the velocity at the centre for different hydraulic gradients, for Soil B, uncoated column. Also shown is the Darcy velocity v_d , calculated from the flow rate measured at the column exit. These velocities were calculated from the times taken for the dye to pass through 90 mm depth of soil. The ratio of v_d to v_{centre} is an estimate of the porosity, n . Figure 8 accordingly gives a porosity value for soil B of 0.43. This compares to a value of $n = 0.40$ (for both soils B and C) obtained by dry density measurement. Similarly for soil C, the estimated porosity from the ratio of v_d to v_{centre} , shown in Fig. 9, is 0.45. The corresponding void ratios for soils B and C, calculated from these porosities of 0.43 and 0.45, are 0.75 and 0.82 respectively.

In both soils, the ratio of the slopes $v_{\text{edge}}/v_{\text{centre}}$ is greater than 1. The plume shape which is consistent with this is represented diagrammatically in Fig. 10. The depth to which the wall effect penetrates into the column is exaggerated in this diagram.

The permeability, k , (hydraulic conductivity) is related to the porosity by the Kozeny-Carmen equation (Bear, 1972).

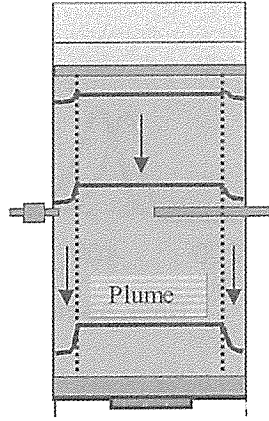


Fig. 10. Diagrammatic plume shape

$$k = \frac{\rho g}{\mu} \left[\frac{n^3}{(1-n)^2} \right] \left(\frac{d_m^2}{180} \right) \quad (1)$$

Where ρ equals density; μ equals viscosity; d_m is a representative particle size.

The average velocity, v , is proportional to k/n :

$$v = \frac{k}{n} i \quad (2)$$

From Eq.(1) k/n is proportional to $n^2/(1-n)^2$, i.e. proportional to e^2 . Assuming that the porosity n varies from n_{centre} at the centre to n_{edge} at the edge, from these equations, in terms of void ratio, e , k/n is proportional to e^2 .

$$\text{As } v_{\text{edge}} = (k_e/n_e) i_{\text{edge}} \quad (3)$$

where v_{edge} is the velocity at the edge

$$v_{\text{centre}} = (k_c/n_c) i_{\text{centre}} \quad (4)$$

$$\text{And } i_{\text{edge}} = i_{\text{centre}}$$

$$\text{then } v_{\text{edge}} / v_{\text{centre}} = (e_{\text{edge}}/e_{\text{centre}})^2 \quad (5)$$

From Fig. 8 and Fig. 9 we know that the edge to centre velocity ratio for Soil B is 1.45 and 1.11 for soil C. Therefore the values of $e_{\text{edge}}/e_{\text{centre}}$ is expected to be the square roots of these: 1.2 and 1.06 respectively, suggesting that the edge - centre void ratio difference increases with particle size.

A theory for boundary effects which considered regular packings of uniform sized particles has already been investigated by Hardin (1989). He defined an equivalent boundary layer of loose packing in order to correct the measured void ratio of soils compacted into containers. For graded soils, in an enclosing container, Hardin found that the voids ratio of the undisturbed core, e_c , differed from the overall voids ratio, e_o , by:

$$e_c = e_o - \frac{1.6 d_{10}}{6V/A} \quad (6)$$

Where d_{10} is the particle size of the 10% fraction of the smallest soil grains, and V and A are the soil volume and area respectively. Applying this concept to a cylindrical flow column in which the boundary layer is a cylindrical "sleeve", requires some judgement. In this case, Hardin's empirical relation may be written:

$$e_c = e_o - \frac{1.6 d_{10}}{1.5D} = e_o - \frac{1.07 d_{10}}{D} \quad (7)$$

where D is the diameter of the column.

Furthermore, the thickness of the boundary layer might be taken, following Hardin's concept of disturbed packing, to be twice the d_{10} particle size. It can then be shown that a column of central core voids ratio, $= 0.75$, would have an overall voids ratio, according to Equation 7, of 0.755. The overall voids ratio, e_o , is equal to the total volume of voids in core plus boundary (edge), divided by the total volume of solids in the core plus boundary (edge):

$$e_o = \frac{\frac{e_c}{1 + e_c} + \frac{e_e}{1 + e_c} \left[\frac{D}{8d} - 1 \right]}{\frac{1}{1 + e_c} + \frac{1}{1 + e_c} \left[\frac{D}{8d} - 1 \right]} \quad (8)$$

This small overall increase, when applied over the small volume of the boundary layer, can be shown to require an edge voids ratio, $e_e = 0.872$. In that case we find that $(e_e/e_c)^2 = 1.35$. This corresponds reasonably with the value of 1.45 interpreted from the flow velocities in Fig. 8. This would be consistent with the boundary layer extending into the soil for only 1 or 2 particle diameters away from the wall. Typical soil grains used are shown in Fig. 11 and 12, where they appear to differ only in size rather than shape.

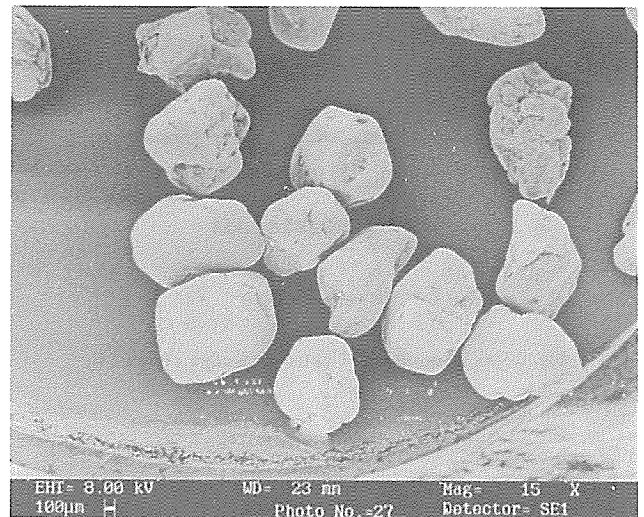


Fig. 11. Fraction B grains

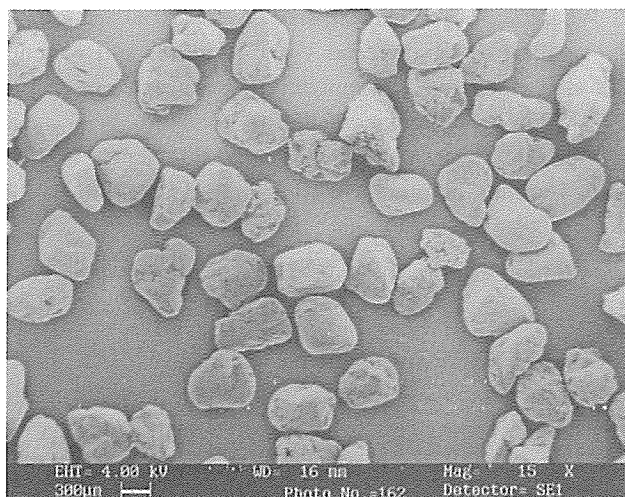


Fig. 12. Fraction C grains

Results with transmission-type sensor

In another series of Soil B experiments, the transmission sensor (Mark 4) was periodically moved across the diameter of the column, to measure the difference in plume delay. Again, in clean unmodified columns the plume travelled faster near the wall (see Fig. 10). The sensor at the edge was the reflective probe. The time delay between the arrival of the plume peak concentration in the measurements above was: Fig. 13(a) 119 seconds, Fig. 13(b) 46 seconds, and Fig. 13(c) 4 seconds, respectively. These results agree with those of the uncoated column above, in that the edge plume leads the centre plume for uncoated walls. The plume shape as well as the time of arrival is identical for the two different sensors, when both are mounted at the edge of the column.

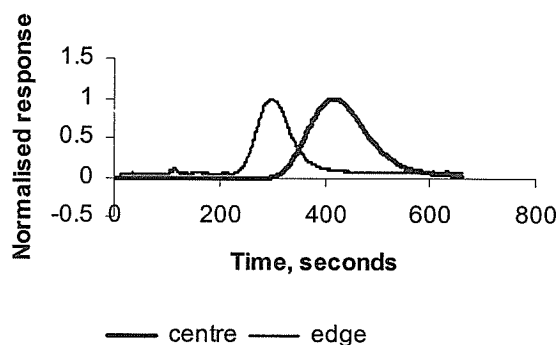


Fig. 13(a). Sensors at Centre and edge of column

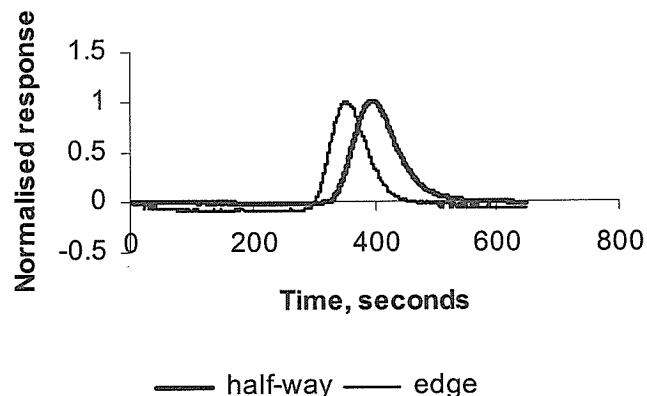


Fig. 13(b). Sensors at Centre and mid-way between centre and edge

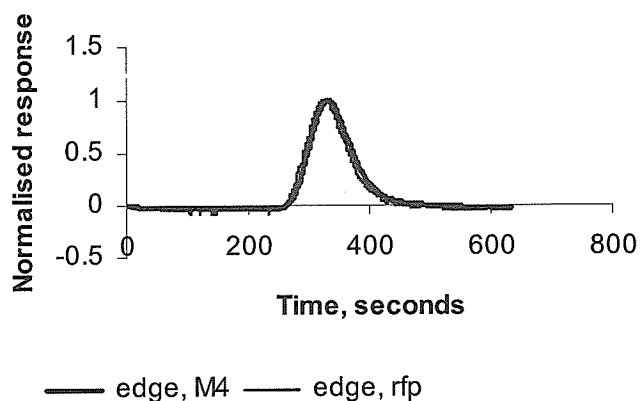
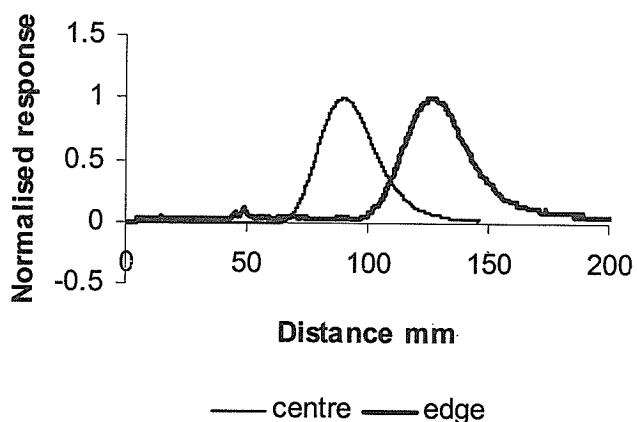


Fig. 13(c). Both sensors at edge of column

To obtain dimensions of the plume, if the data of Fig. 13(a) is transposed from response vs. time to response vs. distance by multiplying time by the velocity at the column centre, the plume profiles shown in Fig. 14 are obtained. Only the plume position has advanced at the wall, and the plume width appears to be constant.

Fig. 14. Plume shape at the sensor position, 90 mm from top, at $t = 418$ seconds

CONCLUSIONS

In-situ fibre-optic sensors have been used successfully to measure the time difference of plume arrival at the edge and in the centre of a soil column. As expected, these results show evidence of an increased void ratio at the edge, where the plume of dye moves faster at the soil column wall boundary.

When the inside wall of the soil container was roughened by coating with sand, the previously seen boundary effect is reduced.

The void ratios at the edge were estimated to be 20% larger than those at the column centre, for sand of particle size range 0.6-1.2 mm, and 6% larger for sand of particle size range 0.3-0.6 mm.

ACKNOWLEDGMENTS

We are grateful to The European Union for a post-doctoral research assistantship for Philippe Sentenac, under TMR grant: NECER, Contract: FMRX-CT96-0030 DG12-ORGS. Thanks are also due to Dr Jacques Garnier (LCPC) for supplying the Comiti and Renaud reference, to Steve Chandler and Tim Ablett for mechanical technical support, and to Gary Bailey for electronics assistance.

REFERENCES

- 1) Bear, J. (1972): "Dynamics of fluids in porous media," American Elsevier, New York.
- 2) Budhu, M. (1991): "The permeability of soils with organic fluids," *Can. Geotech. Journal*, Vol. 28, pp. 140-147.
- 3) Comiti, J. and Renaud, M. (1989): "A new model for determining mean structure parameters of fixed beds from pressure drop measurements, with application to beds packed with parallelepipedal particles," *Chemical Engineering Science*, 44, No. 7, pp. 1539-1545.
- 4) Daniel, D.E., Anderson, D.C., and Boynton, S.S. (1985): "Fixed wall vs flexible wall permeameters," *Hydraulic barriers in soil and rock*, ASTM, STP 874, pp. 107-126.
- 5) Hardin, B. (1989): "Effect of rigid boundaries on measurement of particle concentration," *ASTM Geotechnical Testing Journal*, Vol. 12, No. 2, pp. 143-149.
- 6) Lynch, R.J., Treadaway, A.C.J., Bailey, G., Bolton, M.D., Chandler, S.G., Collison, C.H., Sentenac, P., Garrett, J.A., Santos, C.A., and Silva, M.A.G. (2000): "Fibre-optic photometric probes for tracking groundwater pollutant tracers in geotechnical centrifuge studies," *Proceedings Int. Symp. on Physical Modelling and Testing in Environmental Geotechnics*, La Baule, France, May, pp. 35-42.
- 7) Lynch, R.J., Allersma, H., Braker, H., Bezuijen, A., Bolton, M.D., Cartwright, M., Davies, M.C.R., Depountis, N., Esposito, G., Garnier, J., de Allneida Garrett, J.L.L. Harris, C., Kechavarzi, C., Oung, O., da Silva, M.A.G., Santos, C., Sentenac, P., Soga, K., Spiessl, S., Taylor, R.N., Treadaway, A.C.J., Weststrate, F. (2001) "Development of sensors, probes and imaging techniques for pollutant monitoring in geo-environmental model tests," *International Journal of Physical Modelling in Geotechnics*, Vol. 1, No. 4, pp. 17-27.
- 8) Poorooshasb, F. and Schofield, A.N. (1988): "Pollution migration at 500 gravities," Cambridge University Engineering Dept. Technical Report CUED/D/-Soils TR212.
- 9) Spiessl, S.M. and Taylor, R.N. (2000): "Physical modelling and Testing in Environmental Geotechnics," LCPC, Paris. *Proceedings of Int. Symp. on Physical modelling and Testing in Environmental Geotechnics*, La Baule, France, May, pp. 325-333.
- 10) Treadaway, A.C.J., Lynch, R.J. and Bolton, M.D. (1997): "Pollution transport studies using an in-situ fibre-optic photometric sensor," *Geoenvironmental Engineering*, Yong, R.N. and Thomas, H.R. (eds), Thomas Telford Publ., London, pp. 151-60. Also *Engineering Geology* 53, 195-204, (1998).
- 11) Treadaway, A.C.J., Lynch, R.J., Bolton, M.D. and Barker, H. (1998): "Pollutant tracking with in-situ photometric sensors in a geotechnical centrifuge," *Environmental Geotechnics*, *Proceedings of Third International Congress on Environmental Geotechnics*, Lisbon, September pp. 441-446.

